Nano Energy (2015) 11, 19–27

Available online at www.sciencedirect.com

ScienceDirect

journal homepage: www.elsevier.com/locate/nanoenergy

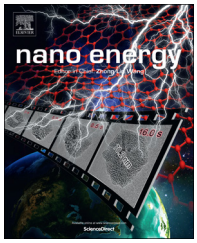

RAPID COMMUNICATION

Hierarchical TiO_2 nanowire/graphite fiber photoelectrocatalysis setup powered by a wind-driven nanogenerator: A highly efficient photoelectrocatalytic device entirely based on renewable energy

Xin Yu[a,1], Xun Han[a,1], Zhenhuan Zhao[b], Jian Zhang[a], Weibo Guo[a], Caofeng Pan[a,*], Aixue Li[a,**], Hong Liu[a,b,***], Zhong Lin Wang[a]

[a]*Beijing Institute of Nanoenergy and Nanosystems, Chinese Academy of Science, Beijing 100083, China*
[b]*State Key Laboratory of Crystal Materials, Shandong University, Jinan 250100, China*

Received 22 August 2014; received in revised form 9 September 2014; accepted 9 September 2014
Available online 28 October 2014

KEYWORDS
Photocatalytic;
Nanogenerator;
TiO_2 nanowire;
Graphite fiber

Abstract
Photoelectrocatalysis is an efficient approach for the degradation of organic pollutants as well as for water splitting. However, an external power source supplying a direct current (DC) is essential to enhance the separation of photo-induced carriers. In this paper, a fully-functional photoelectrocatalysis device was constructed by connecting single crystalline TiO_2 nanowires assembled on graphite microfibers (TiO_2 nanowire/graphite fiber, TNGF) to a wind-driven triboelectric nanogenerator (WDTENG). The excellent photocatalytic and photoelectrocatalytic properties of TNGF originate from the ability of graphite fibers to transport rapidly the charge carriers, the high photocatalytic activity of TiO_2 nanowires and the photo-induced carrier separation enhancement created by the zero band gap of graphite. When this system is used for hydrogen generation via photoelectrocatalytic water splitting, the hydrogen evolution of the TNGF is significantly increased under assistance of the WDTENG. Photoelectrochemical analysis demonstrates that the separation and recombination of photo-induced charge carriers in the 7TNGF composite is dependent on the applied voltage bias. Thus, the wind driven generator

*Corresponding author.
**Corresponding author.
***Corresponding author at: Beijing Institute of Nanoenergy and Nanosystems, Chinese Academy of Science, Beijing 100083, China.
E-mail addresses: cfpan@binn.cas.cn (C. Pan), liaixue@binn.cas.cn (A. Li), hliu@binn.cas.cn (H. Liu).
[1]These authors contributed equally to this work.

http://dx.doi.org/10.1016/j.nanoen.2014.09.024

provides large enough voltage bias for efficient charge separation, leading to a highly enhanced photocatalytic performance. This work is the first instance of high performance photoelectrocatalysis device aimed either at depollution or at hydrogen production which is entirely based on renewable energy.

Introduction

The rapid technological development as well as the demographic expansion of our world is responsible for a series of imminent environmental problems as well as an ineluctable energy crisis. The use of photocatalytic processes either for the degradation of contaminants in water or for the generation of hydrogen as clean fuel is a very practical and effective approach to alleviate these problems [1]. Therefore, it is urgent to develop highly active photocatalysts coupled to efficient photocatalysis techniques [2]. However, most of the existing photocatalysts still suffer from high recombination rate of the photo-induced charge carriers, which largely limits the photocatalytic performance. Separating such carriers is one of the key elements to achieve high photocatalytic efficiency [3]. The main factors causing this recombination process are thought to be related to the presence of crystal defects and to low transfer rates [4]. The concentration of electrons and holes significantly decreases due to the trapping of the charge carriers by the defects whereas low carrier mobilities associated to short diffusion lengths induce fast recombination rates. The presence of defects can be minimized through the improvement of the crystallinity, for example by growing single-crystalline nanomaterials. Recent works have shown that heterostructured nanomaterials constructed with different semiconductor or semiconductor/metal nanoparticles can promote photo-induced carrier separation based on p-n heterojunction [5], Schottky heterojunction [6] and band structure matching physical mechanism [7]. Most recently, a new methodology for enhanced separation of photo-induced carriers was proposed by applying a small electric field to drive the positive or negative charge out of the structure and suppress the recombination process [8]. However, most photoelectrocatalytic devices are based on a film-like working electrode, which is built by coating a layer of photocatalytic powder at the surface of a conductive substrate/electrode. This configuration leads to two obvious flaws. First, the semiconductor nanoparticles are just in physical contact with the surface of the electrode, the electrode – photocatalytic film contact resistivity is too large and it impedes the charge transfer. Second, the film-like geometry of the photocatalytic layer offers only a low surface area which is insufficient to promote high activity, as the reaction is confined to a 2-D and not a 3-D environment.

TiO_2 has been widely used in the fields of solar cell, photocatalysis, gas sensor and biosensor because of its low cost, high chemical stability and environmental friendliness [9]. TiO_2 possesses a wide bandgap of about 3.2 eV and thus excellent photocatalytic activity under UV light illumination [10]. Normally, the use of single phase crystalline TiO_2 nanoparticles as photocatalyst is hampered by photo-induced carrier recombination. As mentioned above, assembling TiO_2 nanoparticles on an conductive substrate is a practical method to enhance the separation of photo-induced carriers by a photoelectrocatalysis technique [11]. In 1972, Fujishima and Honda discovered the phenomenon of photocatalytic splitting of water under a certain bias [12]. Up to now, the most popular photoelectrocatalysis method consists in coating the TiO_2 powder at the surface of conductive metal [8] to form a working electrode, and in applying a constant direct voltage to export photo-induced electrons from the photocatalyst to the electrode, leaving the holes to oxidize the organic pollutant or the water in the case of water splitting [13]. It has been confirmed that under a certain bias, TiO_2 electrodes as anodes can photodegrade formic acid [14], 4-chlorophenol [15], as well as dyes and other organics. Although functional, the efficiency of this two dimensional TiO_2 coated electrode remains low because the photodegradation reaction only occurs at the surface of the electrode. Therefore, it is necessary to develop 3-D stereo photoelectrocatalysts for highly efficient photodegradation and hydrogen generation via water splitting.

As a nontoxic, eco-friendly, low-cost, electrically conductive and chemically and physically stable one-dimensional material, graphite fibers have been used in dye-sensitized solar cells [16], supercapacitors [17], and biosensors [18]. Because graphite fibers are highly graphitized materials with a graphite content higher than 99% [19], they possess numerous advantages compared to amorphous carbon fibers. These advantages make graphite fibers an ideal building block for constructing hierarchical nanostructures for energy storage and photo-electronic transfer materials, in which the electron transfer can be significantly speeded up due to the high electric conductivity of the graphite fibers. Furthermore, their good mechanical properties make them excellent candidates to efficiently support nanostructured catalysts which can be recycled and reused. Therefore, we envision that assembling TiO_2 nanoparticles on graphite micro-fibers to form graphite–TiO_2 nanostructure arrays should lead to high performance photocatalysts.

Most recently, triboelectric nanogenerators (TENG) [20], with their ability to harvest energy from the environment, have attracted much attention because they are easily fabricated, very reliable and efficient, they offer a large output power, and they are low-cost [21]. TENG driven by renewable energy sources, such as light wind [22], water flow [23] and even body movement [24] have been designed and realized. For photoelectrocatalysis, if electricity can be supplied by a wind-driven nanogenerator, systems aiming at the degradation of organic pollutants or the generation of hydrogen should be self-powered. This strategy is efficient and simple, and the resulting device becomes portable and

low-cost as the need for an external power supplier becomes unnecessary.

In this paper, a TiO_2 nanowire/graphite fiber (TNGF) heterostructured hybrid photocatalyst with enhanced photocatalytic performance was synthesized by an in situ hydrothermal synthesis route of single crystalline TiO_2 nanowires at the surface of graphite fibers. At the same time, a wind-driven triboelectric nanogenerator (WDTENG) was prepared for electricity supply. A 3-D stereo photoelectrocatalysis system was designed and realized by connecting TiO_2/graphite microfiber arrays to the wind-driven nanogenerator. To our knowledge, this is the first instance of a photelectrocatalytic system which is based on wind and solar light, two renewable energy sources, without any external power source. Due to its portability, its small size and its autonomy, such device should find a wide range of application, for example in remote areas, in embarked systems or for sensor miniaturization.

Results and discussion

Using X-ray powder diffraction (XRD), it was determined that the crystalline phase of graphite fiber is graphite and the TiO_2 nanowires (either individual or in TNGF) are constituted of rutile (see Supplement materials Figure S1). The microstructure of the as-prepared TiO_2 nanostructures and TNGF hierarchical nanostructures synthesized by hydrothermal method was characterized by scanning electron microscopy (SEM), as shown in Figure 1. The as-synthesized TiO_2 powder is constituted of TiO_2 nanowires self-assembled into flower-like nanostructures (Figure 1a). The nanowires are uniform with length about 400–600 nm, width about 10–20 nm and sharp ends (Figure 1b). As shown in Figure 1c, the graphite fiber has a very smooth surface with a diameter of about 5 μm. Figure 1d shows the SEM image of the TNGF hybrid fibers. The graphite fiber is densely covered with a layer of TiO_2 nanowires with uniform size. The high resolution image of the surface of TNGF shows that the diameter and length of the TiO_2 nanowire is about 10–20 nm and 400–600 nm, respectively, which is similar to the TiO_2 nanowires synthesized in the absence of graphite. The in situ assembled TiO_2 nanowires are uniformly anchored onto the graphite fiber surface. The small size and homogeneous distribution of TiO_2 nanowires may largely increase the effective surface area available for the photocatalytic reaction. Meanwhile, the gaps among the nanowires favor electrolyte transport and molecular diffusion.

Figure 2 shows the typical transmission electron microscopic (TEM) images of TiO_2 nanowires scrapped from the surface of the TNGF. It can be seen that the diameter of the nanowire is about 10–15 nm, which is consistent with the result from SEM. The HRTEM image and the Fast Fourier Transformation (FFT) diffraction pattern show clear crystalline lattice fringe, in agreement with the high crystalline degree of the assembled TiO_2 nanowires. The spacing of the crystalline lattice was determined to be 0.325 nm, which can be indexed to the (110) crystal plane of rutile, indicating that the growth occurs along with the [001] direction [9]. That is to say, the TiO_2 nanowire grows with its [001] direction orthogonal to the surface of the graphite fiber.

To evaluate the photocatalytic, electrochemical catalytic, and photoelectrocatalytic degradation capability of TNGF, we examined the degradation of methyl orange (MO) in water under UV light irradiation as a function of time and 0.8 V potential as external potential (Figure 3). As control experiment, MO was photodegraded by graphite fibers alone or by TiO_2 nanowires alone. It can be seen from Figure 3a, that MO is not degraded under UV irradiation by pure graphite fibers, indicating that graphite fibers have no photocatalytic properties. For the pure TiO_2 nanowires, in 60 min about 50% of MO is degraded under UV light irradiation. Surprisingly, for the TNGF hybrid fibers, the photocatalytic performance is significantly increased and MO can be completely degraded within 60 min, although the total amount of active photocatalyst (TiO_2) in the TNGF hybrid fibers (1.55 mg) is smaller than in the TiO_2 nanowire sample (2 mg). In Figure 3b, the electrochemical degradation of MO under 0.8 V is compared for a bundle of bare graphite and the TNGF hybrid fiber array. By applying 0.8 V of bias voltage between the bare graphite fibers electrode and the counter electrode in dark condition, the MO degradation percentage after 6 h is less than 10%. However, for the TNGF hybrid fibers, under similar conditions, the percentage of MO degradation approaches 70%, which is 7 times greater. Figure 3c shows the photoelectrocatalytic performance of bare graphite fibers and TNGF hybrid fibers at 0.8 V bias voltage and under UV irradiation. After 40 min reaction, there is no obvious degradation of MO for bare graphite, whereas MO has been totally degraded for TNGF hybrid fibers, which illustrates their high performance when used as photoelectrocatalytic electrode materials.

Figure 4 shows the recyclability of TNGF in photocatalysis and photoelectrocatalysis. As shown in Figure 4a, the TNGF hybrid photocatalyst can degrade MO within 60 min. After 4 cycles, the photodegradation activity of TNGF remains as high as in the first cycle, which indicates that the recyclability of TNGF is excellent. Under 0.8 V of bias voltage (Figure 4b), the catalyst can degrade MO within 40 min, which is 20 min shorter than the degradation time without applied bias voltage. After 4 cycles of photoelectrocatalysis process, the catalyst keeps its performance, and no any deterioration of the activity is observed. It suggests that TNGF hybrid fiber is not only a good photocatalyst, but also a promising photoelectrocatalyst.

Based on the above results, we can propose two possible reasons to explain the enhanced photocatalytic and photoelectrocatalyst activity and stability of TNGF. Graphite is a typical zero bandgap material with very high conductivity, which traps photo-induced electrons at the interface of graphite–TiO_2 heterostructures [25]. This process in TNGF enhances the separation of photo-induced carriers in comparison to pure TiO_2 nanowires. Although the heterostructures can prevent the recombination of photo-induced carriers, it is not enough to ensure that most of the photo-induced electrons transfer to graphite because the length of the TiO_2 nanowire is over 500 nm. Bias potential in this system can overcome this problem. The applied voltage induces an electrostatic field, which produce a layer of static positive charge on the surface of graphite fiber electrode. The electrostatic field enforces the photo-induced electrons flow to graphite, and enhances the photo-induced carrier separation.

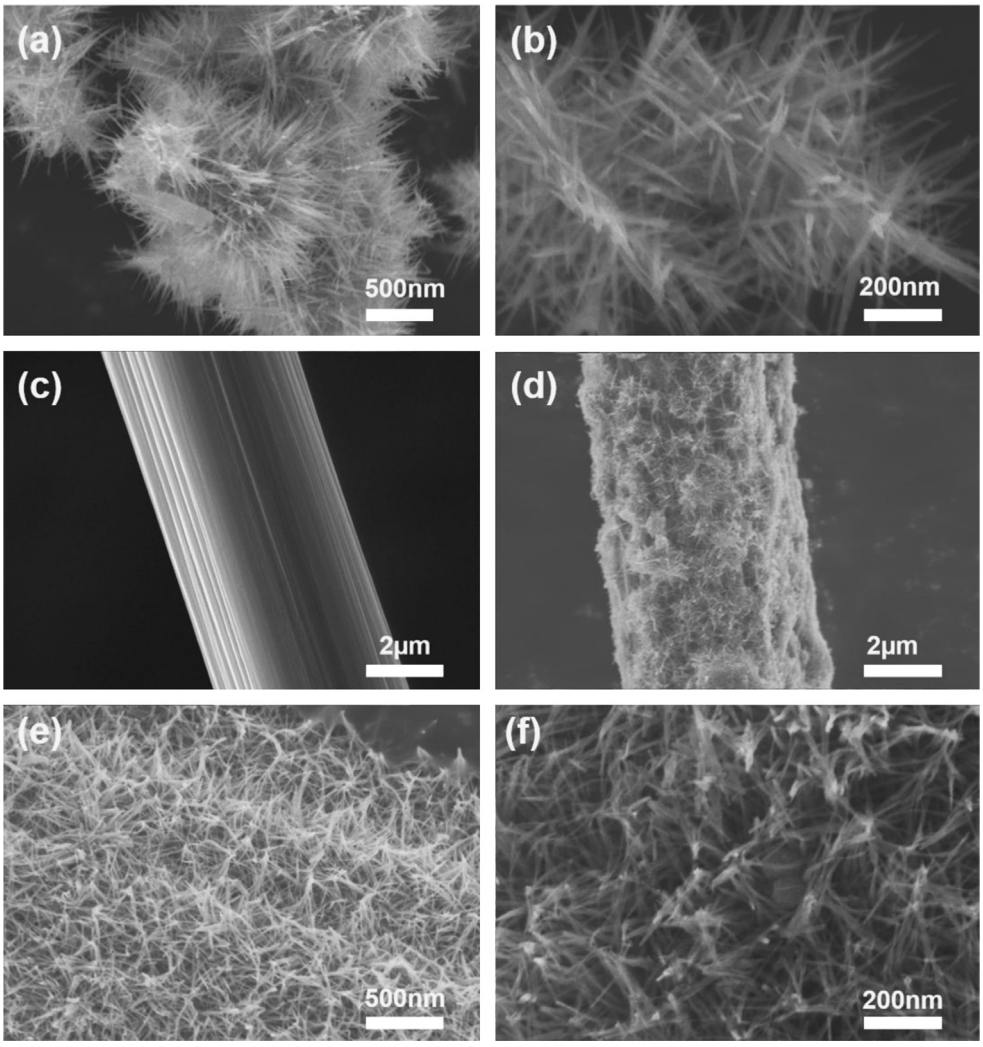

Figure 1 SEM images of (a, b) TiO_2 nanowires (c) graphite fiber, (d) TNGF hierarchical structure, and (e) and (f) high resolution images of TiO_2 nanowires on surface of TNGF.

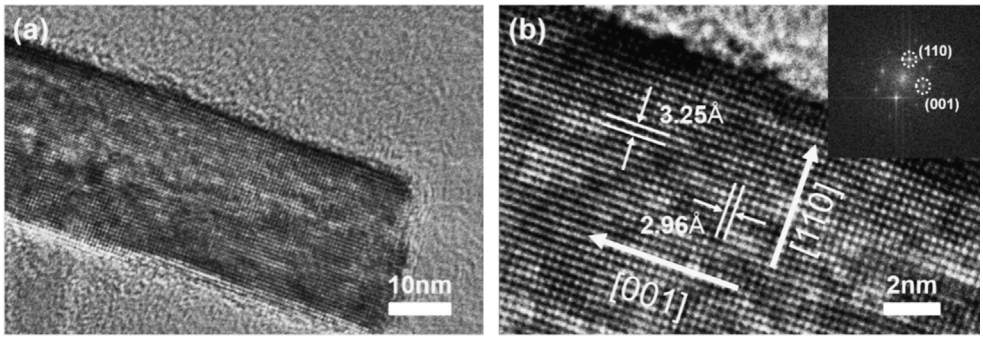

Figure 2 (a) TEM image of TiO_2 nanowires on the surface of the graphite fibers, and (b) HRTEM image of TiO_2 nanowires on the surface of the graphite fibers and Fourier transform electron diffraction pattern of TiO_2 (inset).

Although TNGF is intrinsically able to catalyze the degradation of MO (2–3% after 40 min in darkness under 0.8 V bias voltage, Figure 3c), its activity is very low, unless the reaction is performed under UV irradiation. Therefore, the enhancement of photocatalytic activity for TNGF originates from the electrostatic separation of photo-induced electrons, and not from an electrochemical degradation mechanism [26].

The structure of the TiO_2 nanowire was also tailored in order to favor high photocatalytic activity. The TiO_2 nanowire was grown along the [001] direction with its (110) plane exposed, which is the main reason for the high intrinsic photocatalytic property. It has been proved that for rutile, high energy facets such as {111} and {110} facets possess superior activity in photocatalytic oxidation, and

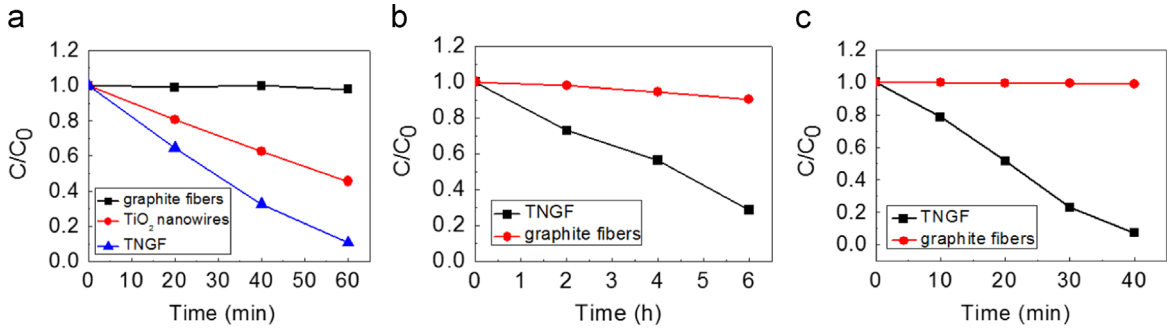

Figure 3 Degradation degree of MO using TNGF and graphite fibers as catalysts at different conditions, (a) photocatalytic degradation under UV light illumination, (b) electrocatalytic degradation of MO with an applied bias of 0.8 V, and (c) photoelectrocatalytic degradation with UV light irradiation at 0.8 V bias.

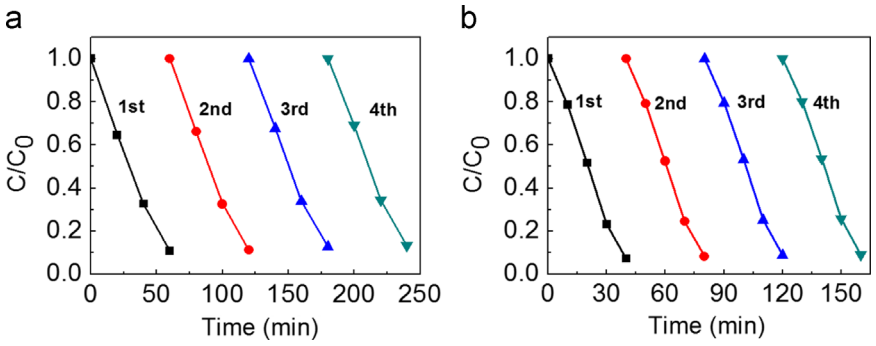

Figure 4 Photocatalytic degradation in recycle experiments under (a) UV light irradiation, and (b) UV light irradiation with 0.8 V bias.

{1 1 0} facets usually act as reductive sites to trap electrons [27]. The nanowires at the surface of the graphite fibers possess high photocatalytic activity due to the predominance of photocatalytic active facets {110}. In addition, it should be pointed out that most of the TiO_2 nanowires are perpendicular to the surface of the graphite fiber, a geometry which facilitates the charge transfer once electron-hole pairs are photogenerated. The small diameter of the nanowire (about 20 nm) is within the mean diffusion length of the charge carriers thus allowing the photo-induced charge carriers to jump at the surface of TiO_2 nanowire for photoreaction. TiO_2 nanowires are densely grown at the surface of the graphite fiber, thus conferring the heterostructures large specific surface area. This set of factors warrants that the hierarchical graphite-TiO_2 nanowire heterostructure has a high photocatalytic activity [28].

As mentioned above, a bias voltage is essential for the TNGF hybrid photocatalyst to be highly active. Most often, a conventional external electric power supply based on fossil fuel is used, thus defeating the very purpose of using solar illumination to fuel the catalyst. In our work, a clean source of energy, namely a wind-driven triboelectric nanogenerator, was used as an electric supplier to apply a bias voltage between the working electrode and the counter electrode. The detailed structure, working mechanism, and demonstration video of the wind-driven nanogenerator are presented in Supplement materials Figure S4. Figure 5a reveals a schematic diagram of the system for H_2 generation combining the photoelectrocatalysis reaction cell with the nanogenerator. In this system, graphite fibers in TNGF are not only part of photoelectrocatalysis electrode, but also act as macroscopic electrode. Both the graphite electrode of WDTENG and the Pt sheet electrode are connected to outputs of the nanogenerator in a parallel circuit. A rectifying bridge circuit was used to convert the alternating-current (AC) output into DC. Figure 5b and Figure 5c shows the output of the WDTENG without a rectifying bridge circuit under a wind speed of about 15.0 m/s. In the cycle of separation-contacting-sliding-separation under wind blowing, the open-circuit voltage (V_{OC}) jumped from zero to a peak value of ~150 V and dropped to zero again. Consequently, the transfer of the charges produced an AC output with a peak short-circuit current (I_{SC}) of ~100 μA corresponding to the vertical contact process.

To demonstrate the photoelectrocatalytic property of TNGF with electricity supplied by a WDTENG, water-splitting and hydrogen generation assays were performed with different fiber materials. Figure 6 shows the H_2 evolution in the system under different conditions for different materials. As shown in curve *a*, there is no H_2 generation for bare graphite fibers under DC and irradiation of Xe lamp, which indicates that bare graphite fibers do not possess any photocatalytic and photoelectrocatalytic property in the absence of TiO_2 nanowires. From curve *b*, we can find that TiO_2 nanowires possess an activity for water splitting as 2 mmol/g of H_2 generation can be obtained after 2 h irradiation with the Xe lamp without applying DC on the sample. Compared to the TiO_2 nanowire, TNGF has a higher activity for water splitting because the separation of the photo-induced carriers is easier, and 3 mmol/g of H_2 can be generated after irradiation with Xe lamp without DC applied

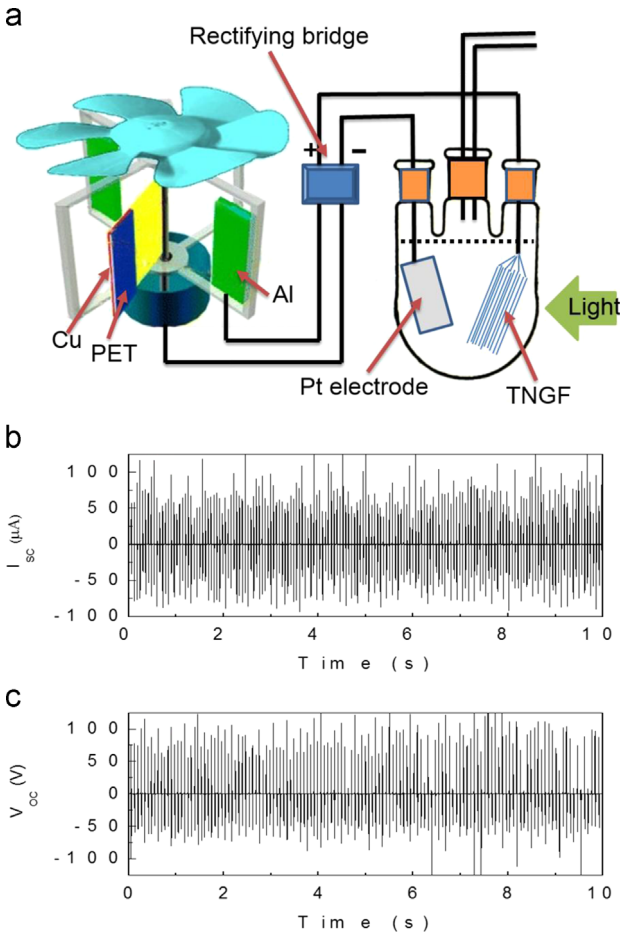

Figure 5 (a) Schematic diagram of WDTENG power assisted photocatalytic H_2 production, (b) the I_{SC} and (c) the V_{OC} of the WDTENG.

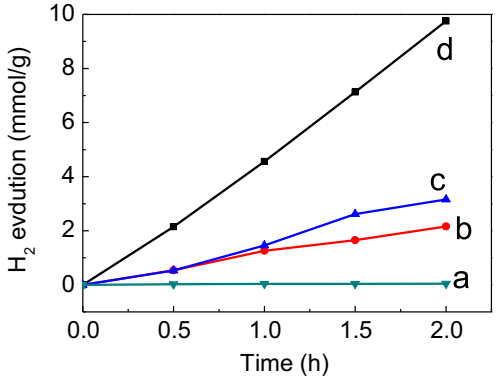

Figure 6 Photoelectrocatalytic hydrogen generation of graphite fiber (curve *a*) and TNGF (curve *d*) under DC provided by WDTENG and white-light, TiO_2 nanowires (curve *b*) and TNGF (curve *c*) under white-light.

(curve *c*). Surprisingly, when DC electricity from WDTENG is applied on the TNGF, H_2 generation increases dramatically, 9.3 mmol/g of H_2 can be generated after 2 h (curve *d*) under the same light irradiation which is over 3 times greater than in the absence of DC. The calculated hydrogen generation rate for the TNGF under light irradiation and with DC from WDTENG (Figure 6) is around 4.87 mmol/(h g), which is much higher than for TNGF without applied electricity (1.46 mmol/(h g)), and then for TiO_2 nanowires under light irradiation without DC (1.24 mmol/(h g)). The H_2 generation rate presented in this work is also significantly greater than the value reported in litterature (1.6 mmol/(h g)) [29].

In order to investigate the effect of the TNGF on the photoelectric behavior, the photocurrents were measured in 0.5 M Na_2SO_4 aqueous solution under simulated sunlight illumination (Figure 7a). For the same applied potential at the TNGF electrode, the current is much larger under illumination than in darkness. Figure 7b presents the photocurrent-time characteristics of the samples at a 0 V bias vs. Ag/AgCl with a 50 s light pulse generated by a Xe lamp. The photo-induced current rises to about 50 μA when the light is on, and drops to 20 μA when the light is off, which illustrates that TNGFs possess a high ability to respond to light. However, no photocurrent can be detected for bare graphite fiber electrode (shown in Figure S6) under the same conditions, which further demonstrates that the photo-induced current flows from TiO_2 nanowires to the surface of TNGFs. The pure TiO_2 nanowire electrode only displayed a very low photocurrent (about 5 μA (Figure S7) under similar conditions). The photocurrent generation is prompt, elevated, and reproducible during each anodic scan which is a consequence of the great optical absorption capability photo-electric coupling property, and excellent separation of photo-generated electrons and holes. The dependence of photocurrent on the applied potential, as shown in Figure 7c, provides important information concerning the photoelectrochemical behavior of the TNGF. The photocurrent vs. time profiles were recorded at −0.1 V, 0 V and 0.3 V vs. Ag/AgCl. When voltage increases, the photocurrent density also increases, which confirms the photo-electric transfer property of the TNGF hybrid fibers.

The hydrogen evolution rate is also strongly dependent on the charge recombination rate which was investigated through the measurement and characterization of transient (time dependent) photocurrent, I_t. A normalized parameter, D [30], can then be calculated using the following equation:

$$D = (I_t - I_{st})/(I_{in} - I_{st})$$

where I_{st} and I_{in} are respectively the steady-state and the initial photocurrents. From the curve $\ln D$ vs. time t (Figure 7d), the transient time constant (τ) can be found at the time for which $\ln D = -1$. For the TNGF (Figure 7d), τ was estimated to be 4.7 s. This long transient time is one of the central reasons behind the very high photocatalytic activity of the TNGF, and it is a proof of the enhanced charge separation process occurring in this material.

Conclusions

TiO_2 nanowire/graphite fiber hybrid three-dimensional nanostructured photocatalysts can be synthesized through a facile hydrothermal process by in situ assembling TiO_2 nanowires on graphite microfibers. The hybrid micro-nano composite photocatalyst possesses high photodegradation performance on MO, and high water splitting property for hydrogen generation which results from the enhancement of the photo-induced carrier separation. Such enhancement originates from the

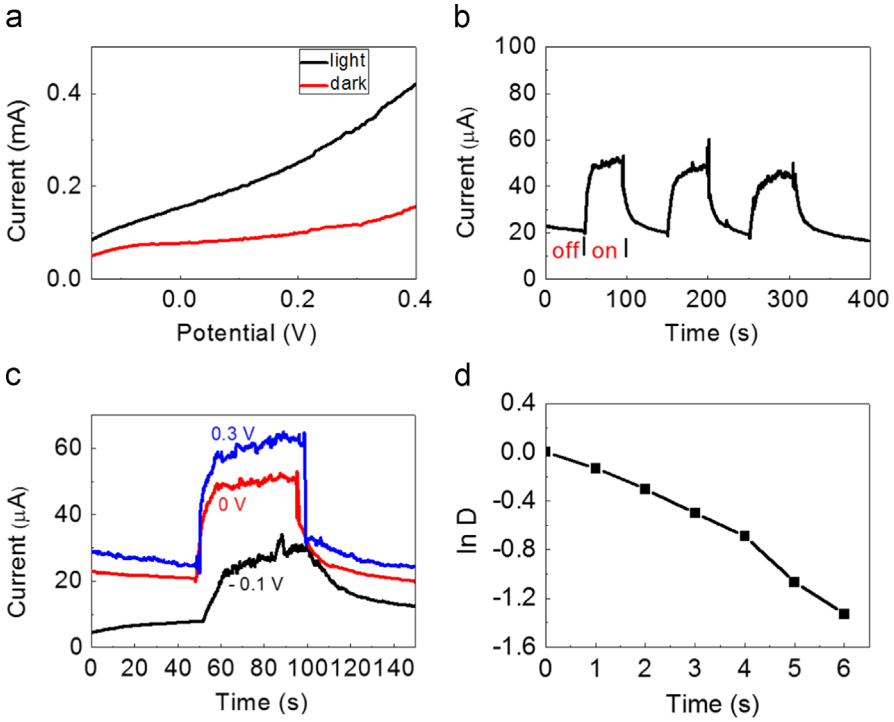

Figure 7 (a) *J*-*V* curves of the TNGF in darkness and under light illumination, (b) on-off *J*-*t* curves of TNGF under 0 V potential, (c) on-off *J*-*t* curves of the TNGF under different potential −0.1 V, 0 V and 0.3 V, and (d) normalized plots of the photocurrent-time dependence of TNGF under 0 V potential.

presence of heterostructures between the zero-bandgap graphite fibers and the semiconductor TiO_2 nanowires containing highly photoactive facet (110) exposed to the solution. Most importantly, the continuous graphite fibers efficiently channel electrons during the photoelectrocatalysis process. By applying a bias voltage, photocatalytic processes are enhanced due to the improved separation of photo-induced electron-hole pairs. As substitution for an external power source, a wind-driven triboelectric nanogenerator can be used to supply electricity. This self-powered device was found to be highly efficient: the rate of H_2 generation under simulated solar illumination and in windy conditions was three times higher than in the absence of wind. For the first time, a self-powered photocatalytic device was operated with no external supply of electricity or any fossil-fuel derived source of energy. Such device is portable and autonomous, which should greatly reinforce the versatility and usefulness of photoelectrocatalysis to alleviate environmental problems. We believe that such systems will have great application in environmental and energy fields, and will encourage the utilization of renewable wind energy to degrade organic pollutants and to produce hydrogen for energy applications.

Experimental section

Materials

All the reagents in this work are of analytic grade and commercially available. Titanium isopropoxide (TTIP), sodium sulfide (Na_2SO_4), ethylene glycol (EG), methanol, urea, hydrochloric acid (HCl), and cetyltrimethyl ammonium bromide (CTAB, $C_{19}H_{42}BrN$) was purchased from China National Medicines Corporation Ltd, and the graphite fibers were purchased from Toray (M40-JB-12K). All the chemicals were used as received without further purification.

Synthesis

TiO_2 nanowire/graphite fiber heterostructured hybrid material were synthesized by a one-step hydrothermal method. In a typical procedure, 0.28 g TTIP was added into 13.80 g concentrated HCl solution (36.0–38.0 wt%) under vigorous stirring to from the TTIP solution. In a separate vessel, CTAB (0.22 g) was added to 27.3 mL of distilled water and stirred for 30 min to form the aqueous CTAB solution. The CTAB solution was added to the TTIP solution and stirred for 1 h resulting in the formation of an aqueous TTIP solution. To 18.75 mL of the TTIP aqueous solution were added 56.25 mL of EG and 0.9 g of urea. After stirring for 1 h, this solution and 20 mg of graphite fibers were transferred to a 100 mL autoclave and heated at 150 °C for 20 h. The collected solid was washed with distilled water 3 times, and dried at 80 °C for 24 h resulting in the formation of the TiO_2 nanowire/graphite fiber hybrid photocatalyst (abbreviated as TNGF). For comparison, TiO_2 nanowires were also prepared in a similar procedure without graphite fiber.

Materials characterization

X-Ray diffractograms of the samples were recorded on an X-ray diffraction spectrometer (D8-advance, BrukerAXS, Germany). The morphology and microstructure of the samples were examined on a scanning electron microscope SEM-a HITACHI S-8020. The TEM images were acquired on a JEOL

JEM 2100 microscope with an operating voltage of 200 kV. The sample for TEM was prepared by dropping a methanol suspension of the sample powder onto a copper microgrid. The sample was thoroughly dried in vacuum prior to observation.

The photocatalytic activity of TNGF was assessed by the photodegradation of MO in a photochemical reaction apparatus. In a typical experiment, 20 mL aqueous suspensions of MO (20 mg/L) and 20 mg of TNGF were placed in a 50 mL beaker. Prior to irradiation, the suspensions were magnetically stirred in the dark for 30 min in order to establish adsorption/desorption equilibrium between the dye and the surface of the catalyst at room temperature. A 300 W mercury lamp with a maximum emission at 356 nm was used as the UV light source. For comparison, photodegradation abilities of 20 mg of graphite fiber and 2 mg of TiO_2 nanowires were evaluated under the same experimental conditions.

The electrocatalytic degradation was conducted using a three-electrode configuration. The TNGF was used as the working electrode and a Pt plate and Ag/AgCl electrode were employed as the counter electrode and reference electrode, respectively. To 40 mL of the 0.5 M Na_2SO_4 electrolyte was added MO at a concentration of 20 mg/L. For the photodegradation of MO under UV light (durability tests of the catalyst), a 300 W mercury lamp with a maximum emission at 356 nm was used as UV light source. At varied irradiation time intervals, the residual MO concentration in the supernatant was analyzed by UV-vis spectroscopic measurement (Shimadzu UV-3600). Four consecutive cycles were performed. The TNGF sample was washed thoroughly with water and dried in between each cycle.

Photoelectrocatalytically water splitting for H_2 generation was conducted in a two-electrode configuration driven with a self-assembled wind driven generator. The positive and negative electrode in the cell was TNGF with a constant weight of 20 mg and a Pt plate, respectively. They were immersed in a solution constituted of 70 mL of water and 30 mL of methanol. A Xe arc lamp with an output power of 300 W was used as white-light source to illuminate the TNGF electrode for 2 h. The power density of the incident light was about 150 mW/cm^2. The produced hydrogen gas was collected and analyzed through an online gas chromatograph.

Photoelectrochemical measurement: A photoelectrochemical cell (PEC) with a three-electrode configuration was constructed. In the PEC, the Pt sheet and Ag/AgCl were used as counter electrode and reference electrode, respectively. Photoelectrochemical performance of the photoelectrode was measured in a 1M NaOH aqueous electrolyte. The electrolyte was bubbled with N_2 for 30 min prior to PEC measurement. The light source was the same as for the photocatalytic production of H_2. The *I-t* curves were recorded under light illumination with an ON-OFF switch programmed at 400 s. The *J-V* curves were obtained with a Gamry electrochemical station (Reference 3000). The scan rate for the linear sweep voltammetry and for the cyclic voltammetry (Figure S5) was 20 mV s^{-1}. Photocurrent stability tests were carried out by measuring the photocurrent produced under chopped light irradiation (light/dark cycles of 50 s) at a fixed electrode potential of 0 V, −0.1 V and 0.3 V vs. Ag/AgCl. During the linear sweep voltammetry (*J-V* plots) and chronoamperometry (stability plots) the electrolyte was continuously bubbled with N_2 to remove oxygen and thus eliminate erroneous signals arising from oxygen reduction.

Acknowledgments

The authors are thankful for fundings from the National Natural Science Foundation of China (Grant no. 51402063), China Postdoctoral Science Foundation (2014M550673), and the “100 Talents Program” of the Chinese Academy of Sciences. Thanks for the support from the "thousands talents" program for pioneer researcher and his innovation team, China.

Appendix A. Supplementary materials

Supplementary data associated with this article can be found in the online version at http://dx.doi.org/10.1016/j.nanoen.2014.09.024.

References

[1] M. Ni, M.K. Leung, D.Y. Leung, K. Sumathy, Renew. Sustain. Energy Rev. 11 (2007) 401–425.
[2] E.W. McFarland, H. Metiu, Chem. Rev. 113 (2013) 4391–4427.
[3] U.I. Gaya, A.H. Abdullah, J. Photochem. Photobiol. C: Photochem. Rev. 9 (2008) 1–12.
[4] M.R. Hoffmann, S.T. Martin, W. Choi, D.W. Bahnemann, Chem. Rev. 95 (1995) 69–96.
[5] J. Lin, J. Shen, R. Wang, J. Cui, W. Zhou, P. Hu, D. Liu, H. Liu, J. Wang, R.I. Boughton, J. Mater. Chem. 21 (2011) 5106–5113.
[6] W. Zhou, D. Wang, H. Liu, J. Wang, Sci. Adv. Mater. 6 (2014) 538–544.
[7] Z. Zhao, H. Liu, S. Chen, Nanoscale 4 (2012) 7301–7308.
[8] Z. Liu, X. Zhang, S. Nishimoto, M. Jin, D.A. Tryk, T. Murakami, A. Fujishima, J. Phys. Chem. C 112 (2008) 253–259.
[9] Z. Sun, J.H. Kim, Y. Zhao, F. Bijarbooneh, V. Malgras, Y. Lee, Y.-M. Kang, S.X. Dou, J. Am. Chem. Soc. 133 (2011) 19314–19317.
[10] T.L. Thompson, J.T. Yates, Chem. Rev. 106 (2006) 4428–4453.
[11] X. Quan, S. Yang, X. Ruan, H. Zhao, Environ. Sci. Technol. 39 (2005) 3770–3775.
[12] A. Fujishima, Nature 238 (1972) 37–38.
[13] K. Vinodgopal, S. Hotchandani, P.V. Kamat, J. Phys. Chem. 97 (1993) 9040–9044.
[14] D.H. Kim, M.A. Anderson, Environ. Sci. Technol. 28 (1994) 479–483.
[15] K. Vinodgopal, U. Stafford, K.A. Gray, P.V. Kamat, J. Phys. Chem. 98 (1994) 6797–6803.
[16] X. Cai, H. Wu, S. Hou, M. Peng, X. Yu, D. Zou, ChemSusChem (2013).
[17] E. Frackowiak, F. Beguin, Carbon 39 (2001) 937–950.
[18] K. Saetia, J.M. Schnorr, M.M. Mannarino, S.Y. Kim, G.C. Rutledge, T.M. Swager, P.T. Hammond, Adv. Funct. Mater. 24 (2014) 492–502.
[19] J. Delmonte, Technology of Carbon and Graphite Fiber Composites, Van Nostrand Reinhold, New York, 1981.
[20] F.-R. Fan, Z.-Q. Tian, Z. Lin Wang, Nano Energy 1 (2012) 328–334.
[21] Z.L. Wang, Acs Nano 7 (2013) 9533–9557.
[22] Y. Xie, S. Wang, L. Lin, Q. Jing, Z.-H. Lin, S. Niu, Z. Wu, Z.L. Wang, Acs Nano 7 (2013) 7119–7125.
[23] Z.H. Lin, G. Cheng, L. Lin, S. Lee, Z.L. Wang, Angew. Chem. Int. Ed. 52 (2013) 12545–12549.
[24] R. Yang, Y. Qin, C. Li, G. Zhu, Z.L. Wang, Nano. Lett. 9 (2009) 1201–1205.
[25] L.W. Zhang, H.B. Fu, Y.F. Zhu, Adv. Funct. Mater. 18 (2008) 2180–2189.

[26] Y. Alivov, M. Pandikunta, S. Nikishin, Z. Fan, Nanotechnology 20 (2009) 225602.
[27] X. Liu, H. Zhang, X. Yao, T. An, P. Liu, Y. Wang, F. Peng, A. R. Carroll, H. Zhao, Nano Res. 5 (2012) 762–769.
[28] P. Salvador, J. Appl. Phys. 55 (1984) 2977–2985.
[29] W. Zhou, Z. Yin, Y. Du, X. Huang, Z. Zeng, Z. Fan, H. Liu, J. Wang, H. Zhang, Small. 9 (2013) 140–147.
[30] F. Meng, J. Li, S.K. Cushing, M. Zhi, N. Wu, J. Am. Chem. Soc. 135 (2013) 10286–10289.

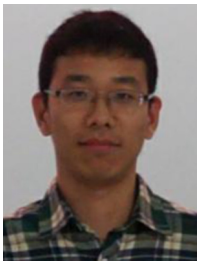

Xin Yu received his undergraduate degree from Hebei University of Technology in 2012. Currently he is pursuing his Ph.D. under the supervision of Prof. Hong Liu at Beijing Institute of Nanoenergy and Nanosystems, Chinese Academy of Science. His research is mainly focused on nanomaterials for photocatalysis and photoeletrocatalysis.

Xun Han received his undergraduate degree from Shandong University in 2012. Currently he is pursuing his Ph.D. under the supervision of Prof. Caofeng Pan at Beijing Institute of Nanoenergy and Nanosystems, Chinese Academy of Science. His research is mainly focused on piezotronics and piezophototronics and their applications in human-electronics interfacing.

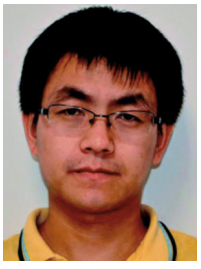

Zhenhuan Zhao received his M.Sc. degree from Shandong Polytechnic University in 2011. Currently he is pursuing his Ph.D. under the supervision of Prof. Hong Liu at the State Key Laboratory of Crystal Materials in Shandong University, China. He is also a joint student at Beijing Institute of Nanoenergy and Nanosystems, Chinese Academy of Sciences. His research is mainly focused on nanomaterials for sustainable energy and energy storage based on supercapacitors.

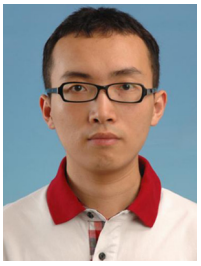

Jian Zhang received her undergraduate degree from Northwestern Polytechnical University in 2012. Currently he is a third-year graduate student of Prof. Hong Liu at Beijing Institute of Nanoenergy and Nanosystems, Chinese Academy of Science. His research is mainly focused on nanomaterials modified graphite fiber for electrochemical.

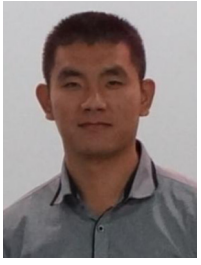

Weibo Guo received his M.Sc. degree from Qingdao University of Science and Technology in 2013. Currently he is pursuing his Ph. D. under the supervision of Prof. Hong Liu in Beijing Institute of Nanoenergy and Nanosystems, Chinese Academy of Science. His research is especially on the application of nanomaterials in tissue engineering.

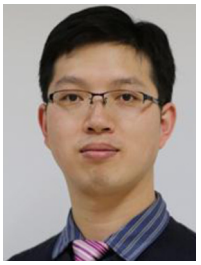

Dr. Caofeng Pan received his B.S. degree (2005) and his Ph.D. (2010) in Materials Science and Engineering from Tsinghua University, China. He then joined in the group of Professor Zhong Lin Wang at the Georgia Institute of Technology as a postdoctoral fellow. He is currently a professor and a group leader at Beijing Institute of Nanoenergy and Nanosystems, Chinese Academy of Sciences since 2013. His main research interests focus on the fields of piezotronics/piezo-phototronics for fabricating new electronic and optoelectronic devices, nano-power source (such as nanofuel cell, nano biofuel cell and nanogenerator), hybrid nanogenerators, and self-powered nanosystems. Details can be found at http://piezotronics.binncas.cn/index%20en.php.

Dr. Aixue Li is an associate professor in Beijing institute of Nanoenergy and Nanosystems, Chinese Academy of Sciences. She received Ph.D. from the state key laboratory of Electroanalytical Chemistry of Changchun Institute of Applied Chemistry, Chinese Academy of Sciences in 2007. Currently, her main interests are focused on biological materials and biosensors.

Dr. Hong Liu is a professor in Beijing Institute of Nanoenergy and Nanosystems, Chinese Academy of Science, and in State Key Laboratory of Crystal Materials, Shandong University. He received his Ph.D. degree in 2001 from Shandong University (China). His current research is focused mainly on tissue engineering, nanomaterials and nanodevices, especially the application of nanomaterials and nanodevices in gas and biosensors, environmental protection, and new energy sources.

Zhong Lin (ZL) Wang received his Ph.D. from Arizona State University in physics. He is now the Hightower Chair in Materials Science and Engineering, Regents' Professor, Engineering Distinguished Professor and Director, Center for Nanostructure Characterization, at Georgia Tech. His discovery and breakthroughs in developing nanogenerators established the principle and technological roadmap for harvesting mechanical energy from the environment and biological systems for powering a personal electronics. His research on selfpowered nanosystems has inspired the worldwide effort in academia and industry for studying energy for micro–nano-systems, which is now a distinct disciplinary in energy research and future sensor networks.